Polymer Chemistry

PAPER

View Article Online
View Journal | View Issue

Cite this: *Polym. Chem.*, 2014, **5**, 5037

Engineering the band gap and energy level of conjugated polymers using a second acceptor unit†

Khalid Mahmood, Heng Lu, Zheng-Ping Liu,* Cuihong Li, Zhen Lu, Xiao Liu, Tao Fang, Qiaohong Peng, Guangwu Li, Lin Li and Zhishan Bo*

Received 2nd January 2014
Accepted 15th April 2014

DOI: 10.1039/c4py00004h

www.rsc.org/polymers

Three novel isoindigo based donor–acceptor (D–A) conjugated polymers **P1–3** have been synthesized by Suzuki polycondensation and utilized as donor materials for polymer solar cells (PSCs). These three polymers are of the same backbone, but have different substituents. All these polymers exhibit high thermal stability and broad absorption in the range of 300 to 770 nm. Hole mobilities of polymer films spin coated from 1,2-dichlorobenzene (DCB) solutions are 7.00×10^{-4}, 2.37×10^{-3} and 2.90×10^{-4} $cm^2\ V^{-1}\ s^{-1}$ for **P1**, **P2** and **P3**, respectively. PSCs based on **P2**:$PC_{71}BM$ (1 : 2 by weight) with a 2% DIO additive displayed a power conversion efficiency (PCE) of 3.41% with a short-circuit current density (J_{sc}) of 7.57 mA cm^{-2}, an open-circuit voltage (V_{oc}) of 0.85 V, and a fill factor (FF) of 53%, under the illumination of AM 1.5G (100 mW cm^{-2}). XRD diffraction measurements have shown that these polymers have a short π–π stacking distance in the solid state. The results demonstrate that these conjugated polymers could be promising donor materials in the application of polymer solar cells.

Introduction

Polymer solar cells have experienced two rapid development periods after the appearance of the bulk heterojunction concept for the active layer and the use of donor–acceptor (D–A) conjugated polymers as the donor materials.[1] The innovations in materials and device structure have boosted the power conversion efficiency (PCE) of PSCs to higher than 10%.[2,3] The active layer of a bulk heterojunction polymer solar cell is a blend of donor and acceptor, which forms an interpenetrated network for highly efficient exciton diffusion and dissociation and the transportation of the formed free charges.[4,5] To achieve high efficiency polymer solar cells, some design criteria of p-type polymer donors are (i) low lying HOMO energy level to increase the open circuit voltage (V_{oc}); (ii) narrow band gap to broaden the absorption range to achieve higher short-circuit current (J_{sc}); (iii) high hole mobility for charge transport. Alternating the D–A approach, which involves the copolymerization of an electron rich monomer with an electron deficient monomer, is the most attractive and successful strategy for controlling the energy level and optical band gap of copolymers through the intramolecular charge transfer from donor to acceptor unit.[6–9] On the basis of this concept, a large number of novel D–A type low band gap polymers have been synthesized and used in PSCs.[7] Carbazole,[10–13] fluorene,[14–16] silafluorene,[17,18] thieno[3,4-*b*]thiophene,[19] and benzo[1,2-*b*:4,5-*b*]dithiophene (BDT)[20–22] are commonly used electron-rich donor units; whereas quinoxaline,[23–25] diketopyrrolopyrrole,[26,27] thienopyrazine,[28,29] benzothiadiazole (BT),[30,31] isoindigo,[32–34] and thieno[3,4-*c*]pyrrole-4,6-dione[35,36] are commonly used electron-deficient acceptor units.

Isoindigo, which is an easily synthesized strong electron withdrawing unit, constitutes a planar moiety capable of forming strong π–π stacks in the solid state. Many isoindigo based D–A alternating conjugated polymers have been synthesized and used for PSC and field effect transistor (FET) applications. The hole and electron mobilities of isoindigo based D–A conjugated polymers have reached 0.81 and 0.66 $cm^2\ V^{-1}\ s^{-1}$, respectively.[37] PSCs based on isoindigo containing D–A conjugated polymers furnished PCEs up to 6.2%.[38]

Among the commonly used acceptor units, BT, which is a widely used planar acceptor unit, can be facilely modified by substitution at the 5- and 6-positions. Many D–A alternating conjugated polymers containing BT have been synthesized and used for PSCs. Especially, D–A alternating conjugated polymers with BT as the acceptor unit, carbazole or fluorene as the donor unit, and thiophene as the spacer have furnished good PSC device performance.[10,39,40] Although the polymer solar cells gave a high open circuit voltage (V_{oc}), the short circuit current (J_{sc}) is still low due to the narrower absorption. To broaden the absorption, BT has been used to polymerize with strong electron donors such as dithienosilole to achieve D–A type conjugated polymers with broad absorption.[41,42] Conjugated polymers based on a strong electron donor unit and BT usually have a

Beijing Key Laboratory of Energy Conversion and Storage Materials, College of Chemistry, Key Laboratory of Theoretical and Computational Photochemistry, Ministry of Education, Beijing Normal University, Beijing 100875, China. E-mail: lzp@bnu.edu.cn; zsbo@bnu.edu.cn; Fax: +86-10-62206891; Tel: +86-10-62207699

† Electronic supplementary information (ESI) available: XRD patterns, ^1H and ^{13}C NMR spectra, output and transfer characteristic curves of blend films and DSC curves. See DOI: 10.1039/c4py00004h

higher HOMO energy level, which is prone to result in lower V_{oc}.[2,3,43–50] To achieve conjugated polymers with broad absorption and a deeper HOMO energy level, we designed and synthesized a series of conjugated polymers containing BT as the acceptor unit, isoindigo as the second acceptor unit, and thiophene as the spacer. As expected, these polymers as thin films exhibit intense and broad absorption and a deep HOMO energy level (<5.44 eV) with a band gap in the range of 1.60–1.63 eV. The highest FET hole mobility can be up to 2.37 × 10^{-3} cm^2 V^{-1} s^{-1}. PSCs have been fabricated with the polymer as the donor and $PC_{71}BM$ as the acceptor. Among these three copolymers, the PSC based on **P2**:$PC_{71}BM$ (1 : 2 by weight) with diiodooctane (DIO) (2% by volume) as the additive showed the best performance with a PCE of 3.41% and a V_{oc} of 0.85 V under an illumination of AM 1.5G (100 mW cm^{-2}).

General procedure for the synthesis of conjugated polymers (P1, P2, and P3)

A mixture of isoindigo based diboronic acid pinacol ester monomer **M4** (0.11 mmol), dibromo monomer **M1–3** (0.11 mmol), toluene, H_2O, and $NaHCO_3$ was carefully degassed before and after $Pd(PPh_3)_4$ was added. The mixture was stirred and refluxed with different reaction times under a nitrogen atmosphere. Phenylboronic acid and $Pd(PPh_3)_4$ were added and refluxed for 4 h; after that bromobenzene was added, and the mixture was refluxed overnight to complete the end-capping reaction. After being cooled to room temperature, water and chlorobenzene were added, and the organic layer was separated and washed three times with water. And then, the solution was heated to 100 °C to dissolve the polymers and filtered. After the removal of most solvent, the residue was poured into a large amount of acetone, and the resulting precipitates were collected by filtration and washed with acetone. The crude product was redissolved in a minimum amount of chlorobenzene and precipitated into a large amount of acetone. The formed precipitates were collected by filtration and dried under high vacuum.

Synthesis of polymer (P1)

M4 (100 mg, 0.11 mmol), **M1** (84 mg, 0.11 mmol), toluene (20 mL), H_2O (2 mL), $NaHCO_3$ (0.2 g, 3.1 mmol), and $Pd(PPh_3)_4$ (1.3 mg, 1.2 μmol) were used for Suzuki polycondensation. Phenylboronic acid (10 mg, 0.08 mmol), $Pd(PPh_3)_4$ (1.3 mg, 1.2 μmol), and bromobenzene (100 μL, 9.55 mmol) were used for the end-capping reaction. **P1** was obtained as a dark blue solid in a yield of 49% (80 mg). ^1H NMR (400 MHz, $CDCl_3$): δ 9.17–9.13 (2H, br), 8.54–8.53 (2H, br), 7.57–7.35 (2H, br), 7.03–6.92 (4H, br), 4.14 (4H, br), 3.78 (4H, br), 1.51–1.18 (64H, br), 0.80–0.79 (12H, br). Anal. calcd for $C_{70}H_{96}N_4O_4S_3$: C 72.87, H 8.39, N 4.86. Found: C 72.16, H 8.41, N 4.87. GPC (PS standards): M_w = 17.9 kg mol^{-1}, M_n = 16.1 kg mol^{-1}, PDI = 1.11.

Synthesis of polymer (P2)

M4 (100 mg, 0.11 mmol), **M2** (80 mg, 0.11 mmol), toluene (20 mL), H_2O (2 mL), $NaHCO_3$ (0.2 g, 3.1 mmol), and $Pd(PPh_3)_4$ (1.3 mg, 1.2 μmol) were used for Suzuki polycondensation. Phenylboronic acid (10 mg, 0.08 mmol), $Pd(PPh_3)_4$ (1.3 mg, 1.2 μmol), and bromobenzene (100 μL, 9.55 mmol) were used for the end-capping reaction. **P2** was obtained as a dark blue solid in a yield of 68% (90 mg). ^1H NMR (400 MHz, $CDCl_3$): δ 9.20–9.18 (2H, br), 8.01–7.93 (2H, br), 7.83–7.81 (2H, br), 6.92–6.90 (4H, br), 3.78–3.77 (4H, br), 2.77–2.61 (8H, br), 1.68–1.45 (24H, br), 1.20–1.16 (36H, br), 0.80–0.78 (12H, br). Anal. calcd for $C_{70}H_{96}N_4O_2S_3$: C 74.95, H 8.63, N 4.99. Found: C 74.81, H 8.68, N 4.95. GPC (PS standards): M_w = 13.2 kg mol^{-1}, M_n = 12.5 kg mol^{-1}, PDI = 1.06.

Synthesis of polymer (P3)

M4 (100 mg, 0.11 mmol), **M3** (85 mg, 0.11 mmol), toluene (20 mL), H_2O (2 mL), and $NaHCO_3$ (0.2 g, 3.1 mmol), and $Pd(PPh_3)_4$ (1.3 mg, 1.2 μmol) were used for Suzuki polycondensation. Phenylboronic acid (10 mg, 0.08 mmol), $Pd(PPh_3)_4$ (1.3 mg, 1.2 μmol), and bromobenzene (100 μL, 9.55 mmol) were used for the end-capping reaction. **P3** was obtained as a dark blue solid in a yield of 42% (60 mg). ^1H NMR (400 MHz, $CDCl_3$): δ 9.20–9.18 (2H, br), 8.14–8.13 (2H, br), 7.32–7.31 (2H, br), 6.92–6.90 (2H, br), 3.78–3.72 (8H, br), 2.79–2.78 (8H, br), 1.68–1.49 (8H, br), 1.21–1.16 (48H, br), 0.80–0.76 (12H, br). Anal. calcd for $C_{70}H_{94}F_2N_4O_2S_3$: C 72.62, H 8.18, N 4.84. Found: C 72.54, H 8.23, N 4.81. GPC (PS standards): M_w = 37.5 kg mol^{-1}, M_n = 21.2 kg mol^{-1}, PDI = 1.77.

Results and discussion

Monomers **M1**,[10] **M2**,[39] **M3**,[51] and **M4** (ref. 52) were synthesized according to the literature procedures and their structure and purity were confirmed by ^1H and ^{13}C NMR spectroscopy and elemental analysis. As outlined in Scheme 1, polymers **P1–3** were synthesized by Suzuki polycondensation of **M1**, **M2**, and **M3** with **M4**, respectively. The polycondensations were conducted in a biphasic mixture of toluene and aqueous $NaHCO_3$ with freshly prepared $Pd(PPh_3)_4$ as the catalyst precursor under a nitrogen atmosphere. After the polymerization, phenylboronic acid and then bromobenzene were successively added at a time interval of 4 h to cap the bromo and boronic acid end groups. After standard workup, **P1**, **P2** and **P3** were obtained in yields of 49%, 68%, and 42%, respectively. **P1** and **P2** showed good solubility in common organic solvents such as $CHCl_3$, chlorobenzene (CB), DCB, and THF. **P3** was only partially soluble in DCB at room temperature, but could be fully dissolved in DCB at elevated temperature. As summarized in Table 1, number average molecular weights (M_n) of the polymers are 16.2 kg mol^{-1} for **P1**, 12.5 kg mol^{-1} for **P2**, and 21.2 kg mol^{-1} for **P3**, with polydispersity indexes (PDIs) of 1.11, 1.06 and 1.77, respectively, measured by gel permeation chromatography (GPC) at room temperature with THF as the eluent and polystyrene as calibration standards.

Thermal properties

Thermal properties of **P1–3** were investigated by thermogravimetric analysis (TGA) and differential scanning calorimetry

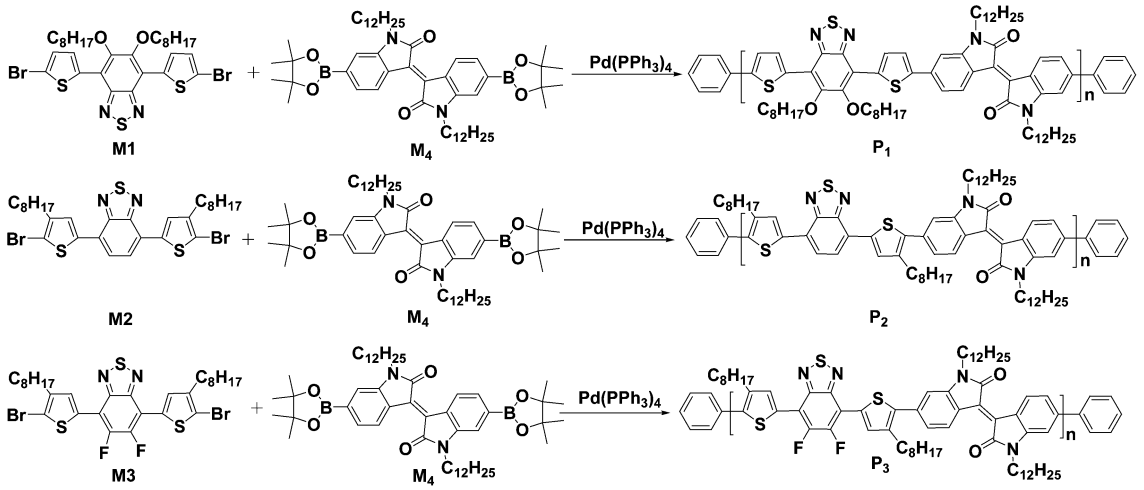

Scheme 1 The synthesis of **P1–3**. Reagents and conditions: $Pd(PPh_3)_4$, toluene, H_2O, $NaHCO_3$, 100 °C, 24–72 h.

Table 1 Molecular weights and thermal properties of the polymers

Polymers	M_n[a] (kDa)	M_w[a] (kDa)	PDI	T_d[b] (°C)	Yield (%)
P1	16.2	17.9	1.11	316	49
P2	12.5	13.2	1.06	438	68
P3	21.2	37.5	1.77	399	42

[a] Determined by GPC using polystyrene standards with THF as the eluent. [b] The 5% weight-loss temperatures under a nitrogen atmosphere.

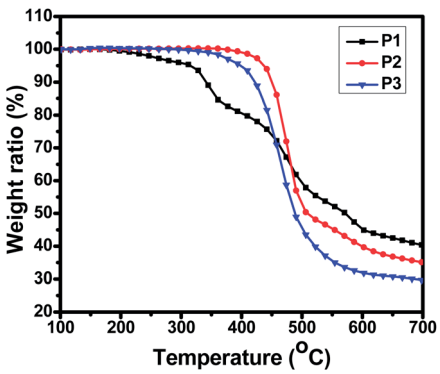

Fig. 1 TGA plots of **P1–3** at a heating rate of 10 °C min^{-1} under a nitrogen atmosphere.

(DSC) at a scanning speed of 10 °C min^{-1} under a nitrogen atmosphere. A 5% mass loss is defined as the thermolysis threshold. As shown in Fig. 1, **P1–3** exhibited good thermal stability and the thermolysis onsets of **P1**, **P2**, and **P3** are located at 316, 438, and 399 °C, respectively. The data are also summarized in Table 1. As shown in Fig. S1 (see ESI),† for all polymers, no noticeable thermal transition was observed from 25 to 300 °C by DSC measurements, which is probably attributed to the stiff backbone that limits the chain motion.

X-ray studies

The packing of polymer chains in the solid state plays a pivotal role in determining the hole mobility of polymer films and the power conversion efficiency of PSCs. Therefore, X-ray diffractions (XRD) of **P1–3** powdery samples were performed to investigate the packing of polymer chains in the solid state and the diffraction patterns are shown in Fig. S2.† **P1** and **P3** exhibited five sharp diffraction peaks; whereas the diffraction peaks for **P2** became weaker and broader. The first peak (d_1), usually denoted as the (100) reflection,[53] at the small angle region can be attributed to the distance the conjugated polymer chains were separated by the two extended alkyl chains. The interchain separation distances are 20.45, 20.75, and 20.11 Å for **P1**, **P2**, and **P3**, respectively. The last diffraction peak (d_2), usually denoted as the (010) diffraction,[53] at the wide angle region probably corresponds to the π–π stacking distance between polymer backbones. The π–π stacking distances are 3.49, 3.61, and 3.47 Å for **P1**, **P2**, and **P3**, respectively. These results indicated that **P1** and **P3** formed a more ordered and closer packing in the solid state than **P2**. The close packing of **P1** and **P3** polymer chains in the solid state is probably due to the following two reasons. For **P1**, the existence of intramolecular S–O interactions endows the polymer backbone with a more planar conformation;[54,55] whereas for **P3**, the existence of fluorine atoms in the polymer backbone usually enhances the interchain interactions and makes the polymer chains pack closer.[56–58]

Optical properties

To access a good deal of information about the electronic structure of polymers, photophysical properties of **P1–3** were investigated by UV-vis-NIR absorption spectroscopy. The absorption spectra of **P1–3** in 1,2-dichlorobenzene (DCB) solutions at room temperature and elevated temperature and as thin films are shown in Fig. 2. As shown in Fig. 2a, **P1** in DCB solution at room temperature exhibited a broad absorption in the visible region with one weak absorption peak located at

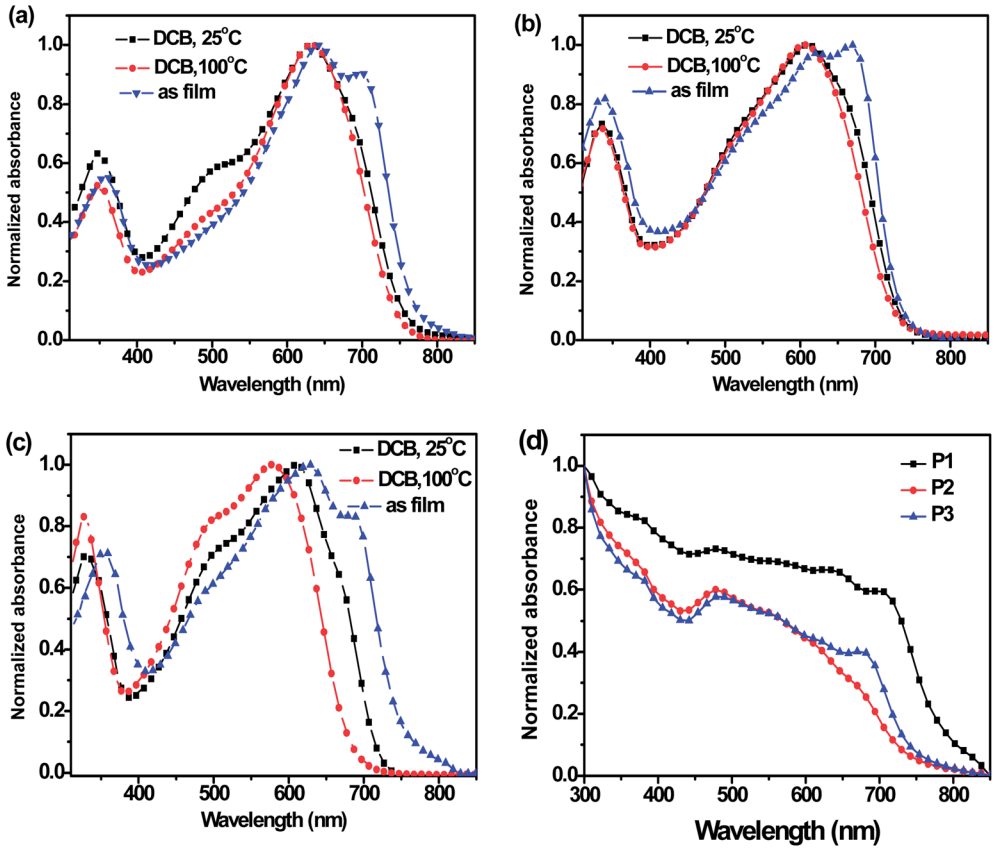

Fig. 2 Normalized UV-vis absorption spectra of **P1** (a), **P2** (b), and **P3** (c) in dichlorobenzene solutions at 25 °C, 100 °C, and as films, respectively, and (d) in the blend films with the ratio of polymer to $PC_{71}BM$ of 1 : 2.

347 nm, one intense absorption peak located at 633 nm, and one shoulder at 496 nm. **P1** in DCB solution at elevated temperature showed almost the same absorption spectrum, only the intensity of the shoulder absorption at 496 nm decreased. Compared with solution absorption spectra, the absorption spectrum of **P1** as a thin film became broader and red-shifted. A new absorption peak at 700 nm appeared, which can be ascribed to the aggregation of polymer chains in the solid state. The absorption spectra of **P2** in DCB solutions at room temperature and elevated temperature are almost the same; whereas the absorption spectrum of **P2** as a thin film is broader and red-shifted with two absorption bands in the long wavelength region with peaks at 621 and 668 nm, respectively, indicating the aggregation of polymer chains in the solid state. **P3** in DCB solution at room temperature displayed a broad absorption in the visible region with two peaks at 331 and 608 nm and a shoulder at 497 nm. At elevated temperature, the absorption spectrum of **P3** in DCB solution is blue shifted and the two peaks are located at 328 and 575 nm, respectively. As a thin film, the absorption spectrum of **P3** is markedly red shifted and broadened and exhibited two absorption peaks located at 627 and 684 nm, respectively, in the long wavelength region. These results indicated that **P1** and **P2** formed real solutions in DCB at room temperature and elevated temperature; whereas **P3** aggregated in DCB solution at room temperature, which can be dissociated at elevated temperature. The high energy band is attributed to the π–π* transition and the low energy band originates from the intramolecular charge transfer (ICT) from

Table 2 Optical and electrochemical properties of three isoindigo-based conjugated polymers

Polymer	Solution λ^a (nm)	Film λ^b (nm)			Oxidation (V, *vs.* Ag/Ag^+ in CH_3CN)	
	λ_{max}^{abs}	λ_{max}^{abs}	λ_{onset}^{abs}	$E_g^{opt\ c}$ (eV)	HOMO (eV)	LUMO (eV)
P1	633, 347	644, 358	775	1.60	−5.44	−3.84
P2	608, 336	668, 338	761	1.63	−5.49	−3.86
P3	575, 328	627, 353	765	1.62	−5.52	−3.90

[a] Measured in dichlorobenzene solution. [b] Thin film spin-coated from chlorobenzene solution. [c] Calculated from the UV absorption band edge of the copolymers film by the equation, $E_g^{opt} = 1240/\lambda_{edge}$.

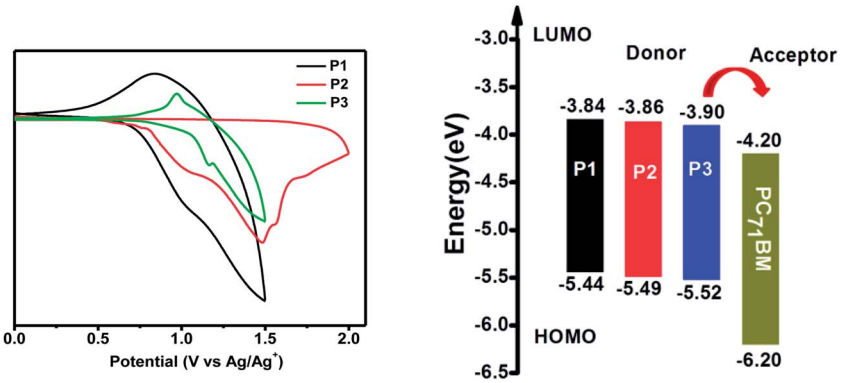

Fig. 3 Cyclic voltammograms (left) of **P1–3** films in 0.1 M Bu_4NPF_6–CH_3CN solutions with a scanning rate of 50 mV s^{-1}. Energy level diagrams (right) for **P1**, **P2**, and **P3** as donor and $PC_{71}BM$ as acceptor.

the donor unit to the acceptor. Optical band gaps (E_g^{opt}) of **P1**, **P2**, and **P3** films estimated from absorption edges of film spectra are 1.60, 1.63, and 1.62 eV, respectively. The narrower band gap of **P1** than that of **P2** and **P3** is probably due to the incorporation of electron donating alkoxy side groups on the benzothiadiazole moiety of **P1**, which elevates the HOMO energy level and decreases the band gap. The broad absorption and small optical band gap make these polymers promising materials for PSCs. The photophysical parameters are also tabulated in Table 2.

Electrochemical properties

Electrochemical properties of **P1–3** were investigated by cyclic voltammetry (CV) with a standard three-electrode electrochemical cell in a 0.1 M tetrabutylammonium hexafluorophosphate ($TBAPF_6$) solution in acetonitrile using polymer films on the Pt working electrode with a scanning rate of 50 mV s^{-1} under a nitrogen atmosphere at room temperature. CV curves of the polymer films are shown in Fig. 3, and the electrochemical data are also summarized in Table 2. HOMO energy levels of **P1**, **P2**, and **P3** were calculated to be −5.44, −5.49 and −5.52 eV, respectively, from the onset of oxidative peaks using the equation $E_{HOMO} = -e(E_{ox} + 4.71)$ (eV), where E_{ox} is the onset oxidation potential in volts. Considering that the open circuit voltage (V_{oc}) of PSCs is correlated to the difference in the LUMO energy level of the acceptor and the HOMO energy level of the donor polymer, the deep HOMO level of **P1–3** is prone to give high V_{oc} PSCs. The two substituents on the benzothiadiazole unit can slightly affect the HOMO energy level of copolymers. The HOMO energy level of non-substituted benzothiadiazole based **P2** is −5.49 eV. **P1** with two electron donating octyloxy substituents on the 5,6-positions of the benzothiadiazole unit showed the highest HOMO energy level of −5.44 eV within these three polymers. The introduction of two electron withdrawing fluoro substituents on the 5,6-positions of the benzothiadiazole unit can lower the HOMO energy level of copolymers. **P3** has the lowest HOMO energy level of −5.52 eV. Therefore a higher V_{oc} is expected for **P3**-based PSCs. According to the equation $E_{LUMO} = E_{HOMO} + E_{bandgap}$, the LUMO energy levels of **P1**, **P2**, and **P3** are calculated to be −3.84, −3.86, and −3.90 eV, respectively.

Field-effect transistor fabrication and characterization

High efficiency polymer solar cells require that the donor–acceptor blend films are of balanced charge carrier mobility. Carrier transport properties of polymers were therefore investigated by fabrication of bottom-gate/top-contact organic thin film field effect transistors (FETs). Thin film FETs were fabricated by spin coating the polymer solutions in 1,2,4-trichlorobenzene (TCB) on the OTS-modified Si/SiO_2 substrates. The as-prepared spin-coated **P1–3** films did not exhibit observable field effects; therefore polymer films, which were subjected to thermal annealing at 160 °C for 30 min, were used for the FET measurements. The output and transfer characteristic curves of **P1**, **P2**, and **P3** films on OTS-treated Si/SiO_2 substrates are shown in Fig. 4. Hole mobilities (μ) of **P1**, **P2**, and **P3** were estimated to be 6.01×10^{-4}, 1.28×10^{-3} and 1.94×10^{-4} cm^2 V^{-1} s^{-1}, respectively, from the derivative plots of the square root of the source–drain current (I_{SD}) *versus* gate voltage (V_G) in the saturated regime through equation $I_{SD} = (W/2L)C_i\mu(V_G - V_T)^2$ where W is the channel width, L is the channel length, C_i is the capacitance per unit area of the gate dielectric layer (SiO_2, 500 nm, $C_i = 7.5$ nF cm^{-2}), and V_T is the threshold voltage. The on/off ratios of **P1**, **P2**, and **P3** based devices are 1.0×10^4, 6.6×10^3, and 6.0×10^3, respectively.

Photovoltaic properties

The broad absorption, narrow band gap, and appropriate HOMO/LUMO energy level make these polymers promising donor materials for BHJ PSCs. Bulk heterojunction solar cells were fabricated with a device structure of glass/ITO/PEDOT:PSS/active layer/LiF/Al. The thicknesses of PEDOT:PSS, LiF, and Al are 40, 0.5, and 100 nm, respectively. Photovoltaic properties of **P1–3** were firstly investigated by blending **P1–3** and $PC_{71}BM$ in DCB in different weight ratios, different concentrations, and different spin-coating speeds. When pure DCB was used as the processing solvent, PSCs with polymer:$PC_{71}BM$ (1 : 2, by weight) as the active layer gave the best device performance. Namely, **P1** based PSCs showed a V_{oc} of 0.78 V, a short circuit current (J_{sc}) of 7.89 mA cm^{-2}, a fill factor (FF) of 0.45, and a power conversion efficiency (PCE) of 2.75%; **P2** based polymer solar cells showed a

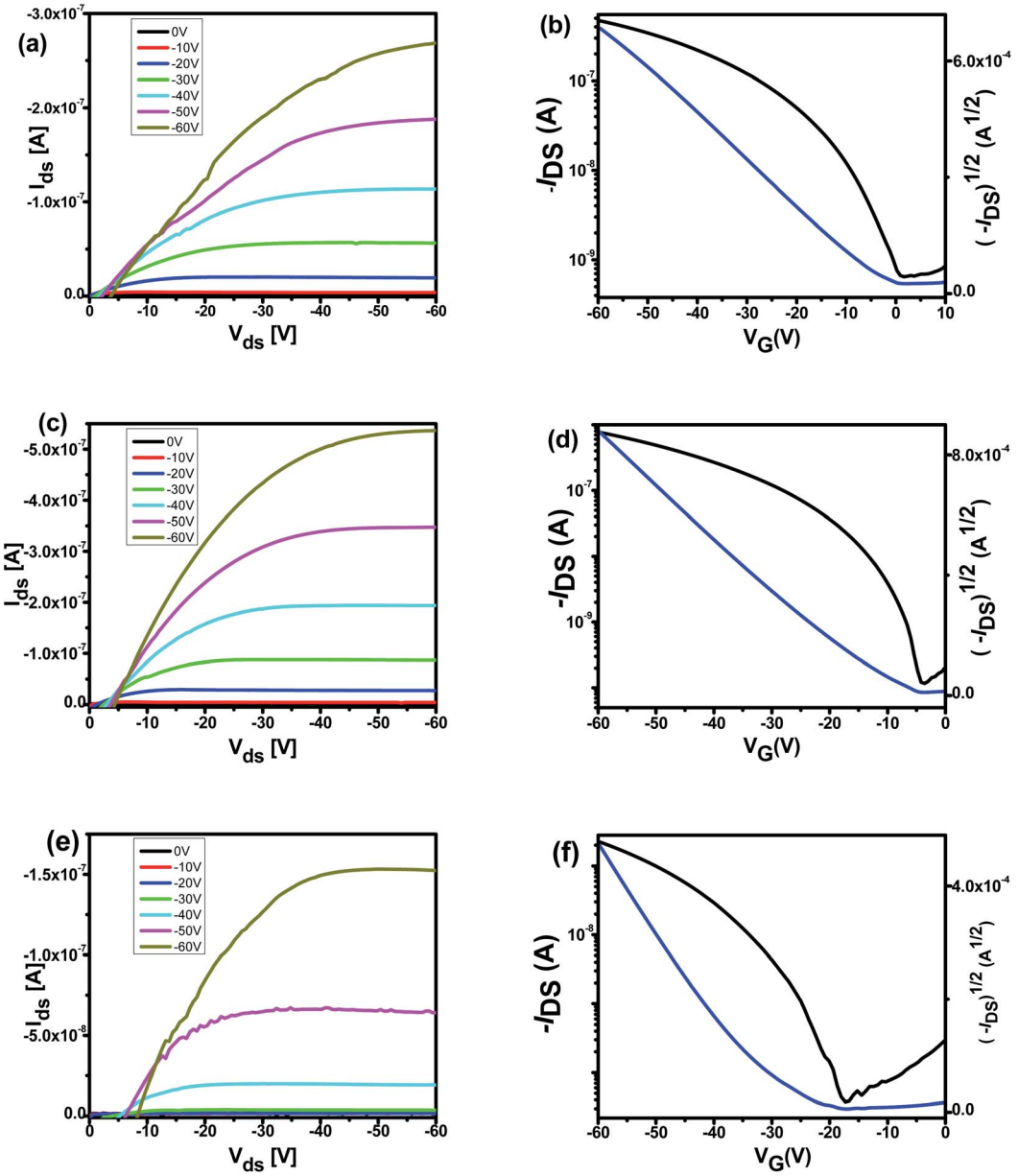

Fig. 4 Output and transfer characteristics of (a and b) **P1**, (c and d) **P2**, and (e and f) **P3** devices (spin-coated from TCB solutions, 10 mg mL^{-1}) at $V_{SD} = -60$ V ($L = 50$ μm, $W = 2.5$ mm) after thermal annealing at 160 °C for 30 min.

V_{oc} of 0.83 V, a J_{sc} of 5.79 mA cm^{-2}, an FF of 0.47, and a PCE of 2.25%; and **P3** based devices showed a V_{oc} of 0.92 V, a J_{sc} of 7.02 mA cm^{-2}, an FF of 0.43, and a PCE of 2.79%. Using 1,8-diiodooctance (DIO) as the additive for DCB, the performance of PSCs can be markedly improved for **P2**, but decreased for **P1** and **P3**. PSCs fabricated with the blend of polymer and $PC_{71}BM$ in a weight ratio of 1 : 2, a blend concentration of 28 mg mL^{-1}, and DCB containing DIO (2.0%, by volume) as the solvent, gave the best performance for **P2**. The highest PCE for **P2** based PSCs reached 3.41% with a J_{sc} of 7.57 mA cm^{-2}, a V_{oc} of 0.85 V, and an FF of 0.53. In contrast to **P2**, PCEs of **P1** and **P3** based PSCs were drastically decreased after the addition of DIO (2.0%, by volume) as an additive. Devices showed a PCE of 1.97% with a J_{sc} of 5.03 mA cm^{-2}, a V_{oc} of 0.76 V, and an FF of 0.51 for **P1** and a PCE of 1.50% with a V_{oc} of 0.78 V, a J_{sc} of 3.58 mA cm^{-2} and an FF of 0.54 for **P3**. The higher V_{oc} of **P3** based PSCs is ascribed to the deepest HOMO energy level of **P3** among these three polymers, due to the strong electron withdrawing effect of the fluorine atoms. Current density–voltage (J–V) curves of the optimized photovoltaic cells are shown in Fig. 5. All devices are tested under 1 sun of simulated AM 1.5G solar radiation (100 mW cm^{-2}) and the data are summarized in Table 3. To evaluate the accuracy of the J_{sc} measurement results, external quantum efficiencies (EQEs) of PSCs were measured under illumination by monochromatic light. As shown in Fig. 5b, PSCs based on **P1–3**:$PC_{71}BM$ (1 : 2, by weight) fabricated without (**P1** and **P3**) and with 2% DIO as additive (**P2**) exhibited a significant broad photoresponse ranging from 400 to 750 nm, which is consistent

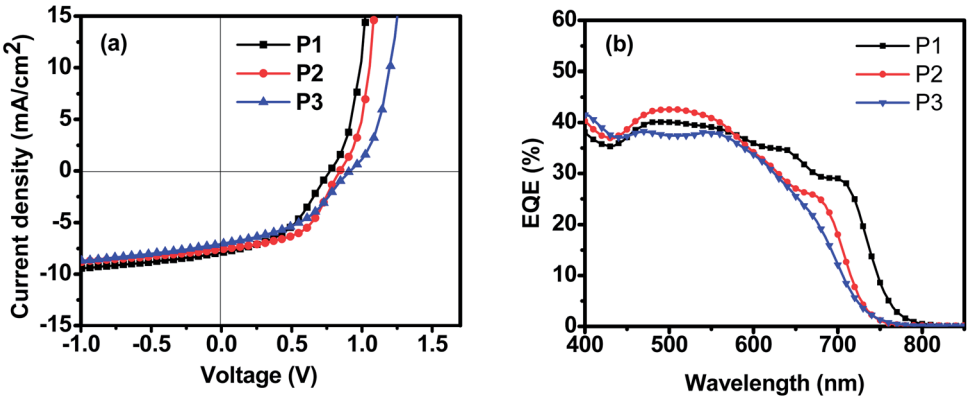

Fig. 5 (a) J–V characteristics of **P1–3**:$PC_{71}BM$ PSCs prepared at a blend ratio of 1 : 2 (by weight) without (**P1** and **P3**) and with DIO (2%, by volume) (**P2**) as the additive; (b) EQE curves of the optimized **P1–3** devices.

with the UV-vis absorption spectra of the blend films shown in Fig. 2d. All current intensity (J_{sc}) values calculated from integration of the EQEs of the devices with an AM 1.5G reference spectrum agreed well with the J_{sc} values obtained from the J–V measurements.

Morphology

The morphology of the active layer is considered to be a key factor that dictates the PCE of PSCs. We used atomic force microscopy (AFM) operating in tapping mode to investigate the surface morphology of the active layer. AFM images of **P1–3**:$PC_{71}BM$ (1 : 2, by weight) blend films spin coated from DCB solutions without or with DIO (2.0%, by volume) are shown in Fig. 6. Without DIO, all the blend films show a rather smooth surface morphology with apparent phase separation as shown in Fig. 6a–c. The root-mean-square (rms) values are 1.93 nm for **P1**, 1.49 nm for **P2**, and 1.20 nm for **P3**. When 2.0% DIO was used as the additive for DCB, the morphology of **P1**:$PC_{71}BM$ and **P3**:$PC_{71}BM$ blend films became apparently rougher, and the domain size got larger. The rms values were increased to 7.25 and 3.64 nm, for **P1** and **P3** based blend films, respectively. The increase in domain size may be responsible for the decrease in the PCE for **P1** and **P3** based PSCs fabricated with the addition of DIO. For **P2**:$PC_{71}BM$ blend films, the addition of 2% DIO only brought about a slight increase in domain size and rms value (1.99 nm). It is apparent that the appropriate phase separation and the decreasing of domain size are favorable for efficient charge separation and transportation in the active layer. AFM results are consistent with the device performances.

Conclusions

In summary, three new D–A type π-conjugated polymers **P1–3** containing two different acceptor units in the polymer main chain have been synthesized and used as donor materials for PSCs. As films, these polymers have a broad absorption ranging from 300 to 750 nm, narrow band gap around 1.60 eV, and deep HOMO energy levels from −5.44 to −5.52 eV. The hole mobilities of **P1–3** films range from 1.94×10^{-4} to 1.28×10^{-3} $cm^2\ V^{-1}\ s^{-1}$. Polymer solar cells fabricated with the blend of **P2**:$PC_{71}BM$ as the active layer using DCB as the solvent and 2.0% DIO as the additive gave the maximum PCE of 3.41% with a J_{sc} of 7.57 mA cm^{-2}, a V_{oc} = 0.85 V, and an FF of 0.53. These results demonstrate that two different acceptor units can be used to construct D–A type conjugated polymers to achieve appropriate energy levels for PSC applications.

Acknowledgements

We express thanks for the financial support by the NSF of China (51003006, 91233205, and 21161160443), the 973 Programs (2011CB935702 and 2009CB623603), and the Fundamental Research Funds for the Central Universities.

Table 3 Device performance of polymer (**P1–P3**):$PC_{71}BM$ at a ratio of 1 : 2 (by weight) devices[a]

Active layer	Solvent	J_{sc} (mA cm^{-2})	V_{oc} (V)	FF	PCE (%)	Thickness (nm)
P1:$PC_{71}BM$	DCB	7.89	0.78	0.45	2.75 (2.66)	113
P1:$PC_{71}BM$	DCB + 2% DIO	5.03	0.76	0.51	1.97 (1.88)	98
P2:$PC_{71}BM$	DCB	5.79	0.83	0.47	2.25 (2.13)	115
P2:$PC_{71}BM$	DCB + 2% DIO	7.57	0.85	0.53	3.41 (3.13)	111
P3:$PC_{71}BM$	DCB	7.02	0.92	0.43	2.79 (2.70)	92
P3:$PC_{71}BM$	DCB + 2% DIO	3.58	0.78	0.54	1.50 (1.40)	109

[a] The average PCE in parentheses were calculated using at least 3 devices for each condition.

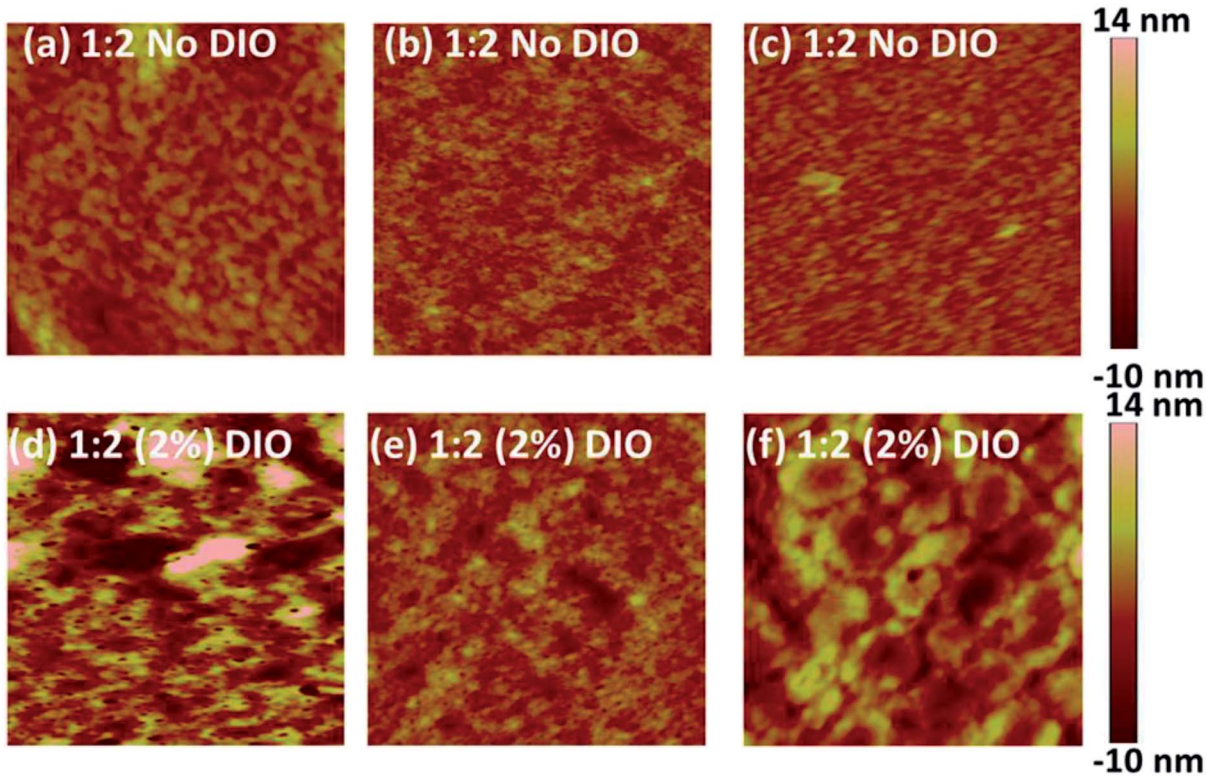

Fig. 6 Tapping mode AFM height images (2 × 2 μm) of (a) **P1**:$PC_{71}BM$, (b) **P2**:$PC_{71}BM$, and (c) **P3**:$PC_{71}BM$ in a weight ratio of 1 : 2 spin coated from DCB solutions; for (d) **P1**:$PC_{71}BM$, (e) **P2**:$PC_{71}BM$, and (f) **P3**:$PC_{71}BM$ with 2% DIO as the additive.

Notes and references

1 S. H. Park, A. Roy, S. Beaupre, S. Cho, N. Coates, J. S. Moon, D. Moses, M. Leclerc, K. Lee and A. J. Heeger, *Nat. Photonics*, 2009, **3**, 297.
2 J. You, L. Dou, K. Yoshimura, T. Kato, K. Ohya, T. Moriarty, K. Emery, C.-C. Chen, J. Gao, G. Li and Y. Yang, *Nat. Commun.*, 2013, **4**, 1446.
3 J. You, C.-C. Chen, Z. Hong, K. Yoshimura, K. Ohya, R. Xu, S. Ye, J. Gao, G. Li and Y. Yang, *Adv. Mater.*, 2013, **25**, 3973.
4 J. Roncali, *Chem. Rev.*, 1997, **97**, 173.
5 A. Ajayaghosh, *Chem. Soc. Rev.*, 2003, **32**, 181.
6 F. C. Krebs, *Sol. Energy Mater. Sol. Cells*, 2009, **93**, 393.
7 J. Chen and Y. Cao, *Acc. Chem. Res.*, 2009, **42**, 1709.
8 C. Li, M. Liu, N. G. Pschirer, M. Baumgarten and K. Müllen, *Chem. Rev.*, 2010, **110**, 6817.
9 Y. Li, *Acc. Chem. Res.*, 2012, **45**, 723.
10 R. Qin, W. Li, C. Li, C. Du, C. Veit, H.-F. Schleiermacher, M. Andersson, Z. Bo, Z. Liu, O. Inganas, U. Wuerfel and F. Zhang, *J. Am. Chem. Soc.*, 2009, **131**, 14612.
11 N. Blouin, A. Michaud and M. Leclerc, *Adv. Mater.*, 2007, **19**, 2295.
12 Y. Zou, D. Gendron, R. Badrou-Aich, A. Najari, Y. Tao and M. Leclerc, *Macromolecules*, 2009, **42**, 2891.
13 K. Mahmood, Z.-P. Liu, C. Li, Z. Lu, T. Fang, X. Liu, J. Zhou, T. Lei, J. Pei and Z. Bo, *Polym. Chem.*, 2013, **4**, 3563.
14 D. Kitazawa, N. Watanabe, S. Yamamoto and J. Tsukamoto, *Appl. Phys. Lett.*, 2009, **95**, 53701.
15 L. J. Lindgren, F. Zhang, M. Andersson, S. Barrau, S. Hellstrom, W. Mammo, E. Perzon, O. Inganas and M. R. Andersson, *Chem. Mater.*, 2009, **21**, 3491.
16 Y. Li, H. Li, B. Xu, Z. Li, F. Chen, D. Feng, J. Zhang and W. Tian, *Polymer*, 2010, **51**, 1786.
17 E. Wang, L. Wang, L. Lan, C. Luo, W. Zhuang, J. Peng and Y. Cao, *Appl. Phys. Lett.*, 2008, **92**, 033307.
18 P.-L. T. Boudreault, A. Michaud and M. Leclerc, *Macromol. Rapid Commun.*, 2007, **28**, 2176.
19 J. Hou, H.-Y. Chen, S. Zhang, R. I. Chen, Y. Yang, Y. Wu and G. Li, *J. Am. Chem. Soc.*, 2009, **131**, 15586.
20 Y. Liang, Z. Xu, J. Xia, S.-T. Tsai, Y. Wu, G. Li, C. Ray and L. Yu, *Adv. Mater.*, 2010, **22**, E135.
21 C. M. Amb, S. Chen, K. R. Graham, J. Subbiah, C. E. Small, F. So and J. R. Reynolds, *J. Am. Chem. Soc.*, 2011, **133**, 10062.
22 H. L. Pan, Y. N. Li, Y. L. Wu, P. Liu, B. S. Ong, S. P. Zhu and G. Xu, *Chem. Mater.*, 2006, **18**, 3237.
23 A. J. Moule, A. Tsami, T. W. Buennagel, M. Forster, N. M. Kronenberg, M. Scharber, M. Koppe, M. Morana, C. J. Brabec, K. Meerholz and U. Scherf, *Chem. Mater.*, 2008, **20**, 4045.
24 F. Zhang, J. Bijleveld, E. Perzon, K. Tvingstedt, S. Barrau, O. Inganäs and M. R. Andersson, *J. Mater. Chem.*, 2008, **18**, 5468.
25 H. Yi, R. G. Johnson, A. Iraqi, D. Mohamad, R. Royce and D. G. Lidzey, *Macromol. Rapid Commun.*, 2008, **29**, 1804.
26 M. M. Wienk, M. Turbiez, J. Gilot and R. A. J. Janssen, *Adv. Mater.*, 2008, **20**, 2556.

27 W. Li, K. H. Hendriks, A. Furlan, W. S. C. Roelofs, M. M. Wienk and R. A. J. Janssen, *J. Am. Chem. Soc.*, 2013, **135**, 18942.
28 A. P. Zoombelt, J. Gilot, M. A. Wienk and R. A. J. Janssen, *Chem. Mater.*, 2009, **21**, 1663.
29 M. H. Petersen, O. Hagemann, K. T. Nielsen, M. Jorgensen and F. C. Krebs, *Sol. Energy Mater. Sol. Cells*, 2007, **91**, 996.
30 E. Bundgaard and F. C. Krebs, *Sol. Energy Mater. Sol. Cells*, 2007, **91**, 954.
31 J. Kim, S. H. Park, S. Cho, Y. Jin, J. Kim, I. Kim, J. S. Lee, J. H. Kim, H. Y. Woo, K. Lee and H. Suh, *Polymer*, 2010, **51**, 390.
32 R. Stalder, J. Mei and J. R. Reynolds, *Macromolecules*, 2010, **43**, 8348.
33 T. Lei, Y. Cao, Y. Fan, C.-J. Liu, S.-C. Yuan and J. Pei, *J. Am. Chem. Soc.*, 2011, **133**, 6099.
34 Z. Ma, E. Wang, M. E. Jarvid, P. Henriksson, O. Inganas, F. Zhang and M. R. Andersson, *J. Mater. Chem.*, 2012, **22**, 2306.
35 Y. Zhang, S. K. Hau, H.-L. Yip, Y. Sun, O. Acton and A. K. Y. Jen, *Chem. Mater.*, 2010, **22**, 2696.
36 Y. Zou, A. Najari, P. Berrouard, S. Beaupre, B. R. Aich, Y. Tao and M. Leclerc, *J. Am. Chem. Soc.*, 2010, **132**, 5330.
37 T. Lei, J.-H. Dou, Z.-J. Ma, C.-J. Liu, J.-Y. Wang and J. Pei, *Chem. Sci.*, 2013, **4**, 2447.
38 E. Wang, Z. Ma, Z. Zhang, K. Vandewal, P. Henriksson, O. Inganas, F. Zhang and M. R. Andersson, *J. Am. Chem. Soc.*, 2011, **133**, 14244.
39 H. Zhou, L. Yang, A. C. Stuart, S. C. Price, S. Liu and W. You, *Angew. Chem., Int. Ed.*, 2011, **50**, 2995.
40 C. Du, C. Li, W. Li, X. Chen, Z. Bo, C. Veit, Z. Ma, U. Wuerfel, H. Zhu, W. Hu and F. Zhang, *Macromolecules*, 2011, **44**, 7617.
41 H.-Y. Chen, J. Hou, A. E. Hayden, H. Yang, K. N. Houk and Y. Yang, *Adv. Mater.*, 2010, **22**, 371.
42 M. C. Scharber, M. Koppe, J. Gao, F. Cordella, M. A. Loi, P. Denk, M. Morana, H.-J. Egelhaaf, K. Forberich, G. Dennler, R. Gaudiana, D. Waller, Z. Zhu, X. Shi and C. J. Brabec, *Adv. Mater.*, 2010, **22**, 367.
43 L. Dou, C.-C. Chen, K. Yoshimura, K. Ohya, W.-H. Chang, J. Gao, Y. Liu, E. Richard and Y. Yang, *Macromolecules*, 2013, **46**, 3384.
44 H. Bronstein, J. M. Frost, A. Hadipour, Y. Kim, C. B. Nielsen, R. S. Ashraf, B. P. Rand, S. Watkins and I. McCulloch, *Chem. Mater.*, 2013, **25**, 277.
45 H. Bronstein, D. S. Leem, R. Hamilton, P. Woebkenberg, S. King, W. Zhang, R. S. Ashraf, M. Heeney, T. D. Anthopoulos, J. de Mello and I. McCulloch, *Macromolecules*, 2011, **44**, 6649.
46 L. Biniek, B. C. Schroeder, J. E. Donaghey, N. Yaacobi-Gross, R. S. Ashraf, Y. W. Soon, C. B. Nielsen, J. R. Durrant, T. D. Anthopoulos and I. McCulloch, *Macromolecules*, 2013, **46**, 727.
47 Y. Zhang, J. Zou, C.-C. Cheuh, H.-L. Yip and A. K. Y. Jen, *Macromolecules*, 2012, **45**, 5427.
48 J. S. Kim, Z. Fei, D. T. James, M. Heeney and J.-S. Kim, *J. Mater. Chem.*, 2012, **22**, 9975.
49 K. W. Song, M. H. Choi, H. J. Song, S. W. Heo, J. Y. Lee and D. K. Moon, *Sol. Energy Mater. Sol. Cells*, 2014, **120**, 303.
50 H. Jun Song, D. Hun Kim, M. Hee Choi, S. Won Heo, J. Young Lee, J. Yong Lee and D. Kyung Moon, *Sol. Energy Mater. Sol. Cells*, 2013, **117**, 285.
51 M. Jayakannan, P. A. van Hal and R. A. J. Janssen, *J. Polym. Sci., Part A: Polym. Chem.*, 2002, **40**, 251.
52 R. Stalder, J. Mei, J. Subbiah, C. Grand, L. A. Estrada, F. So and J. R. Reynolds, *Macromolecules*, 2011, **44**, 6303.
53 F. Liu, C. Wang, J. K. Baral, L. Zhang, J. J. Watkins, A. L. Briseno and T. P. Russell, *J. Am. Chem. Soc.*, 2013, **135**, 19248.
54 E. Q. Jin, C. Du, M. Wang, W. W. Li, C. H. Li, H. D. Wei and Z. S. Bo, *Macromolecules*, 2012, **45**, 7843.
55 J. A. Irvin, I. Schwendeman, Y. Lee, K. A. Abboud and J. R. Reynolds, *J. Polym. Sci., Part A: Polym. Chem.*, 2001, **39**, 2164.
56 A. C. Stuart, J. R. Tumbleston, H. Zhou, W. Li, S. Liu, H. Ade and W. You, *J. Am. Chem. Soc.*, 2013, **135**, 1806.
57 S. C. Price, A. C. Stuart, L. Q. Yang, H. X. Zhou and W. You, *J. Am. Chem. Soc.*, 2011, **133**, 4625–4631.
58 C. Du, W. Li, Y. Duan, C. Li, H. Dong, J. Zhu, W. Hu and Z. Bo, *Polym. Chem.*, 2013, **4**, 2773.